4.1

Orographic Precipitation and Water Vapor Fractionation over the southern Andes

Ronald B. Smith and Jason P. Evans
Yale University
New Haven, Connecticut

1. Introduction

The southern Andes are often mentioned as having the best example of upslope rain and rain shadow effects, with precipitation changing from 6000mm per year on the Chilean coast to less than 300mm in Argentina. According to Prohaska (in Miller, 1976), in southern Chile " The orographic effects are probably as "pure" and simple as can be found anywhere on earth. The range is relatively narrow and oriented perpendicular to the flow. The zone would undoubtedly make an excellent "laboratory" for the verification of theoretical models of air flow over mountain and the resulting precipitation and cloudiness patterns."

The goal of this study is to determine the isotope fractionation of water vapor crossing the southern Andes and to use this information to estimate the drying ratio. The drying ratio is the ratio of the water removed by orographic precipitation to the incoming water vapor flux. We also wish to test and calibrate a physical model of orographic precipitation.

2. Climatology

To establish the wind climate of the region, we used the NCEP/NCAR Reanalysis (Mo and Higgins, 1996). Selecting only rainy days for 2004, the wind rose for coastal Patagonia is shown in Fig 1, for the average winds below 500hPa. It shows clearly the dominance of westerly flow over the region. The average wind speed was 11m/s with a standard deviation of 7m/s. The average wind direction was 273º. Twenty four percent of the time, the wind was westerly. Sixty percent of the time the wind direction fell in the range WSW to WNW. Included in the wind rose are a few cases of rainy easterly flow that we suspect are spurious. The Reanalysis is known to give unphysical drizzle from time to time. The Reanalysis also shows a freezing level between 1 and 2 km, tilting downward as one moves southward.

Corresponding Author Address: Ronald B. Smith, Dept. of geology and geophysics, Yale University, P.O. Box 208109, New Haven CT, 06520; ronald.smith@yale.edu

3. Terrain

These westerly winds encounter a very complex glacially dissected terrain. The view from the west in Fig. 2 is computed from an SRTM dataset smoothed horizontally to one kilometer; reducing the peak altitudes. It shows that on average, the airflow must lift about two kilometers to pass over the southern Andes.

4. Vegetation

A qualitative view of the precipitation pattern is available from the vegetation distribution observed using cloud-removed composite satellite images. . In Figure 3 we show the MODIS-derived annually averaged Normalized Difference Vegetation Index (NDVI). There is a striking contrast between the dense vegetation along the Chilean coast and the barren steppe in Argentina. The North and South Patagonian Ice Fields, the ocean and some isolated snowy peaks show negative NDVI. The intermediate NDVI values in the south west coastal region represent mountain forests that are snow covered during a few winter months.

5. Stream water sample collection and isotope analysis

The measurement of broad scale precipitation isotope gradients across the Andes was carried out by sampling summer "base flow" streamwater (Kendall and Coplen, 2001). Seventy one stream water samples were collected in Patagonia between 22 January and 5 February in 2005. The collection expedition started with a brief leg from Puerto Montt, Chile southwest to Chiloe. Subsequently, the team drove east across the divide to Bariloche, Argentina and south to Los Antiguos along highway 40 in Argentina. Re-crossing the Andes, they drove southwest to the River Nef, and then north along the Carrera Austral to Puerto Aisen, Chaiten and back to Puerto Montt. The collection sites ranged from 40.7 to 46.7 degrees south latitude on both sides of the Andean divide (Fig. 3a). Most of the samples were taken from small streams so that the catchments centroids were near the sample locations. At each site, GPS positions and landscape photographs were recorded. Samples were stored in tightly sealed Vacutainers. An addition, at many sites, small twig samples were taken for water extraction. In the driest

areas of Argentina, in the warm season, the streambeds were dry so that only twig samples could be collected.

In March 2005, the streamwater samples were sent to Iso-Analytical Limited in the UK for hydrogen and oxygen isotope analysis. In June 2005, water was extracted from the tree samples and sent to the same laboratory for isotope analysis. The repeatability of the mass spectrometer analysis can be judged from the standard deviation of delta values from replicates of our two data sets and two sets of standards: i.e. 1.12, 1.31, 1.85 and 2.67 ppt for deuterium, and similarly 0.08, 0.1, 0.1 and 0.09 ppt for oxygen. These small laboratory uncertainties have little if any impact on our analyses as the fractionation by the Andes is nearly one hundred times greater. Sampling errors may be more significant. As expected, there is a strong gradient in measured isotope ratio across the Andes range. Samples from the west have typical $\delta D = -30, \delta^{18}O = -4$ while samples from the east are much "lighter" with $\delta D = -110, \delta^{18}O = -14$.

6. Drying ratio estimates

According to the concept of Rayleigh fractionation, condensation preferentially removes the heavier isotopes so the remaining vapor becomes progressively lighter following

$$R / R_0 = \Theta^{\alpha-1} \qquad (1)$$

where R and R_0 are the ratios of heavy to light isotope concentrations in the final and initial state vapor, Θ is the fraction of water vapor remaining and α is the fractionation coefficient (Friedman, 1953 and Dansgaard, 1964). The condensate at each stage of fractionation will follow a similar rule, so using (1)

$$DR = 1 - \Theta = 1 - (R_P / R_{P0})^{1/(\alpha-1)} \qquad (2)$$

where R_P and R_{P0} are the ratios of heavy to light isotope concentration in the upwind and downwind precipitation. The isotope ratios are represented by the "delta" value, $\delta = (R / R_{VSMOW} - 1) * 1000$, using Vienna Standard Mean Ocean Water (R_{VSMOW}) as a reference.

The fractionation factor in the exponent of (2) is slightly temperature and phase dependent. If the vapor condenses to liquid at T = -10C, the fractionation factor for hydrogen/deuterium is about $\alpha_D = 1.13$ (Friedman and O'Neil,1977). If the heavy and light end points for deuterium are $\delta D_{MAX} = -30$ and $\delta D_{MIN} = -110$ ppt then (2) gives a drying ratio of

$$DR = 1 - (0.890 / 0.970)^{7.69} = 1 - 0.52 = 0.48$$

7. Model prediction of isotope ratio in precipitation

To predict the spatial distribution of isotopes in rainfall over Patagonia we use the linear precipitation model of Smith and Barstad (2004) and the Rayleigh fractionation equation (2). According to the linear model, the precipitation P(x,y) is proportional to the horizontal water vapor flux, given approximately by

$$\vec{F} = \rho q_w \vec{U} H_w \qquad (3)$$

where q_w is the mixing ratio at the ground, H_w is the depth of the moist layer and $\vec{U}$ is the average wind vector. For the present application, the linear model had to be extended to handle the large drying ratio. The model is run on an extended domain (39 to 49S; 69 to 76W) and further embedded in a tapered buffer zone. The model grid increment is one kilometer using smoothed SRTM terrain.

The vapor removed from the airstream is the integral of the precipitation rate along the wind direction

$$I(x,y) = \int_{-\infty}^{x,y} P(x',y')ds \qquad \text{where}$$

$$ds = (Udx' + Vdy') / |\vec{U}| \qquad (4)$$

The fraction removed is the local drying ratio $DR(x,y) = I(x,y) / |\vec{F}_0|$ and the fraction remaining is $\Theta = 1 - DR$. Note that both I(x,y) and F_0 have the same units: $kg \cdot m^{-1} \cdot s^{-1}$.
Using (2), the delta value of the local precipitation is

$$\delta = [(\frac{\delta_0}{1000} + 1)\Theta^{\alpha-1} - 1] \times 1000 \qquad (5)$$

where δ_0 is the delta value of the first upstream rain. If the ocean evaporation and first cloud condensation are reversible so $R_{p0} = R_{VSMOW}$ and $\delta_0 = 0$ then (5) becomes

$$\delta = (\Theta^{\alpha-1} - 1) \times 1000 \qquad (6)$$

As an example, if $\alpha = 1.1$ and $DR = 0.2$, then $\Theta = 0.8$ and $\delta = (.8^{0.1} - 1) \times 1000 = -22$. By using (6) with constant alpha, any latitude effect on the incoming isotope ratio was ignored.

Now imagine that the region is subject to winds and precipitation events with different durations, directions and strengths. These characteristics are used to group

the rain events into classes. The average precipitation rate (during rain events) is given by

$$\overline{P}(x,y) = \sum_i P_i D_i \Big/ \sum_i D_i \qquad (7)$$

where (P_i, D_i) are the precipitation rate and duration for each event class "i". The annual precipitation is the numerator of (7). The average normalized isotope ratio at each point is the mass weighted isotope ratio for each event class. From (6)

$$\overline{\delta}(x,y) = \sum_i \delta_i P_i D_i \Big/ \sum_i P_i D_i \qquad (8)$$

where (δ_i) is the isotope ratio for each class. If an event type produces little precipitation at a point (x,y) then the isotope ratio in that small rainfall event gets little weight in (8).

Using many runs of the linear model, $\overline{P}(x,y)$ from (7) and $\overline{\delta}(x,y)$ from (9) are derived from the terrain, cloud physics and water vapor flux climatology. Both $\overline{P}(x,y)$ and $\overline{\delta}(x,y)$ are invariant regional fields; independent of how many total rainfall events occur.

8. Model tuning

Using the deuterium and oxygen-18 data from the stream water samples taken in 2005, an optimization procedure was carried out to find the best values for parameters in the linear model. Five parameters were varied. The most important parameter was the total cloud delay time. The quality of the fit was computed with the "efficiency" (Lagates and McCabe, 1999).

To illustrate the selectivity of the optimization process, we show several tuning curves in Figure 4. Only the highest fractionation factors are used ($\alpha_D = 1.17$ and $\alpha_O = 1.019$) and the two taus are combined into a "total tau". The tuning curves are rather sharply peaked. The "best" model uses 1mm/day of background precipitation, a 6-point wind-rose and a total tau of 1700 seconds.

9. **Conclusions**

The strong deuterium and oxygen-18 isotope fractionation in precipitation across the southern Andes can be readily measured using either streamwater or sapwater sampling. Both types of samples represent average precipitation over many weeks or months, smoothing over the inter-storm variability. Stream water has the advantage that no extraction is required. Sapwater sampling requires vacuum extraction in the laboratory but it allows higher spatial resolution and extension into dry areas where streambeds are usually empty.

One objective here was to determine the drying ratio for a mountain range without an upper air, radar or dense raingauge network. Isotopes are well suited for this estimation. Using streamwater or sapwater and a Rayleigh model, the fractionation in the southern Andes indicates a maximum airstream drying ratio near to 50%, the largest value yet observed for a mountain range. The DR value is slightly sensitive to assumptions about cloud temperatures and phase.

The second application of isotope data is to test and calibrate a linear model of orographic precipitation. We determined that a total cloud delay time of $\tau_C + \tau_F = 1700$ seconds gives the best fit to the stream water data. These same parameter values give a good fit to the sapwater data also. Isotope data correlate better with the linear model than with simple predictors like altitude, longitude or highest upwind peak.

When the optimized linear model is used to predict precipitation fields in the southern Andes, it gives detailed patterns with sharp hilltop maxima and dry leeside valleys. For example, it predicts 5 to 10 meters of (liquid equivalent) precipitation per year on the Patagonia ice sheets, perhaps in line with recent observations of Shiraiwa et al. (2002)

The present southern hemisphere results are rather similar to the previous northern hemisphere mountain isotope study in Oregon (Smith et al., 2005). There, the isotope values gave a drying ratio of about 43% which in turn constrained the total time delay to be $\tau_C + \tau_F > 1200$ seconds. For the Olympic range in Washington State, Anders (2005) found that precipitation patterns using $\tau_C + \tau_F \approx 1600$ agreed with output from a full numerical model. Other estimates for delay times are given by Barstad and Smith (2005)

One key assumption, in estimating DR from precipitation isotopes and vice versa, is that the precipitation is drawn from a well mixed water vapor reservoir passing aloft. A more robust approach would be to add isotopes to the cloud algorithms in a full numerical model (e.g. Cokk et al, 2003, Jiang and Smith, 2003 or Colle 2004), to obtain an explicit prediction of the precipitation isotope ratio. This approach would take into account altitude dependence of the cloud fractionation process.

10. **Acknowledgements**:
Sigrid R-P. Smith gave valuable assistance in the field. Roland Geerken and Larry Bonneau at the Yale Center for Earth Observation assisted with the satellite image analysis. Alison Anders gave useful comments on the manuscript. Logistical assistance was given by Veronica and Jorge Ayling in Esquel and Isabel Anwandter in Puerto Aisen. Rene Garreaud contributed useful ideas. MODIS and SRTM data were from NASA and USGS. This research was partly supported by the National Science Foundation, Division of Atmospheric Sciences (ATM-0112354,-0531212) and NASA (EOS/03-0587-0425)

11. References

Barstad, I., and R. B. Smith, 2005: Evaluation of an Orographic Precipitation Model. *J. Hydrometeor.*, **6**, 85–99.

Colle, A.B., 2004: Sensitivity of Orographic Precipitation to Changing Ambient Conditions and Terrain Geometries: An Idealized Modeling Perspective. *J. Atmos. Sci.*, **61**, 588–606.

Cook, K. H., X. Yang, C. M. Carter, and B. N. Belcher, 2003: A Modeling system for studying climate controls on mountain glaciers with application to the Patagonian icefields. *Climatic Change*, **56**, 339-367.

Dansgaard, W., 1964: Stable isotopes in precipitation. *Tellus*, **16**, 436-468.

Friedman, I., 1953: Deuterium content of natural waters and other substances. *Geochimca et Cosmochimica Acta*, **4**, 89-103.

Friedman, I, and J. R. O'Neil, 1977: Compilation of stable isotope fractionation factors of geochemical interest.. USGS Prof. Paper 440-KK. U.S. Geological Survey, Reston, VA.

Friedman, I., G. I. Smith, J. D. Gleason, A. Warden, and J. M. Harris, 1992: Stable isotope composition of waters in southeastern California. Part 1: Modern precipitation. *J. Geophys. Res.*, **97,** 5795-5812.

Hoffmann, J.A.J., 1975: *Atlas Climatico de America Sur*. World Meteorological Org., 28 pp.

Jiang, Q. and R. B. Smith. 2003: Cloud timescales and orographic precipitation. *J. Atmos. Sci.*, **60**, 1543–1559.

Kendall, C., and T. B. Coplen, 2001: Distribution of oxygen-18 and deuterium in river waters across the United States. *Hydrol. Processes*, **15**, 1363-1393.

Legates, D. R. and G. J. McCabe, 1999: Evaluating the use of "goodness-of-fit" measures in hydrologic and hydroclimatic model validation. *Water Resour. Res.*, **35**, 233-241.

Miller, A.., 1976: The Climate of Chile. *Climates of Central and South America*: Vol 12, W. Schwerdtfeger, Ed., Elsevier, 113-129.

Mo, K.C. and R. W. Higgins. 1996: Large-scale atmospheric moisture transport as evaluated in the NCEP/NCAR and the NASA/DAO reanalyses. *J. Climate*, **9**, 1531–1545.

Shiraiwa, T., S. Kohshima, R. Uemura, N. Yoshida, S. Matoba, J. Uetake, and M. A.Godoi, 2002: High net accumulation rates at Campo de Hielo Patagonica Sur, South America, revealed by analysis of a 45.97m long ice core. *Ann. Glaciol.*, **35**, 84-90.

Smith, R.B. and I. Barstad. 2004: A linear theory of orographic precipitation**.** *J. Atmos. Sci.*, **61**, 1377–1391.

Smith, R.B., I. Barstad and L. Bonneau. 2005: Orographic precipitation and Oregon's climate transition. *J. Atmos. Sci.*, **62**, 177–191.

Smith, R.B., Q. Jiang, M. Fearon, P. Tabary, M. Dorninger, J. Doyle, and R. Benoit., 2003: Orographic precipitation and airmass transformation: An Alpine example. *Quart. J. Roy. Meteor. Soc.*, **129**, 433-454, Part B.

Smith, R.B., J.P. Evans, 2006, Orographic precipitation and water vapor fractionation over the southern Andes, In Press Journal of Hydrometeorology.

Stern, L. A. and P. M Blisniuk, 2002: Stable isotope composition of precipitation across the southern Patagonian Andes. *J. Geophys. Res.*, **107**, D23, 4667.

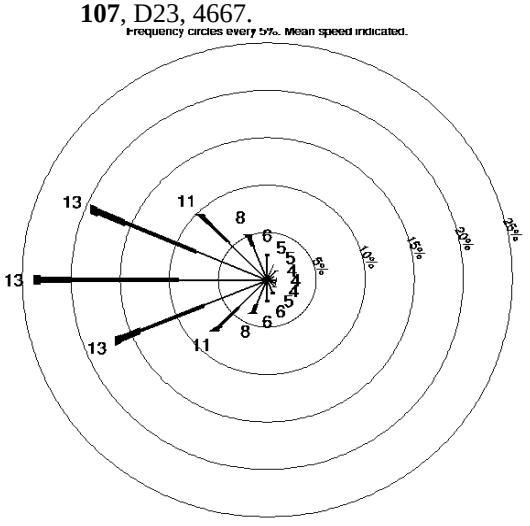

1. Coastal wind rose showing the frequency of occurrence of 16 wind directions and speeds during rain events in the southern Andes. The length of each radial line indicates the percentage of occurrence of that wind direction. Data was obtained from NCEP/NCAR reanalysis mean daily winds for 2005.

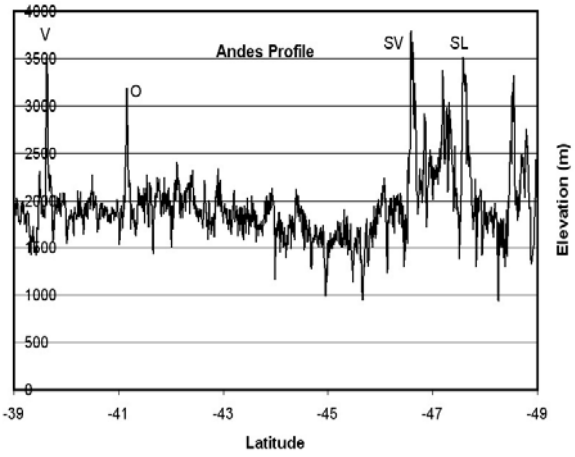

2. The southern Andes profile as seen from the west. The maximum terrain elevation at each latitude is taken from the smoothed one-kilometer SRTM data set. The marked peaks are Villarrica(V), Osorno (O), San Valentin (SV) and San Lorenzo(SL). The Northern Patagonian Ice Field is seen near 47S. Vertical exaggeration is about 200:1.

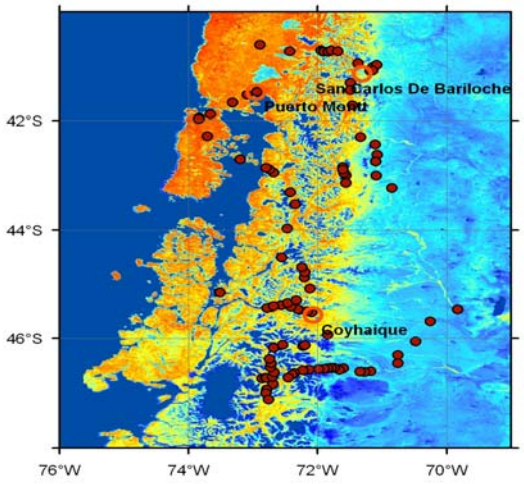

3. The southern Andes vegetation derived from MODIS composite accumulated vegetation (NDVI) distribution. The coastal forests have a high vegetation index (red) while the Argentine steppe has low vegetation (pale blue). The ocean, ice fields and snowy mountain tops have negative NDVI (dark blue). The streamwater sampling sites are shown with circles. Three cities with IAEA data are shown for reference.

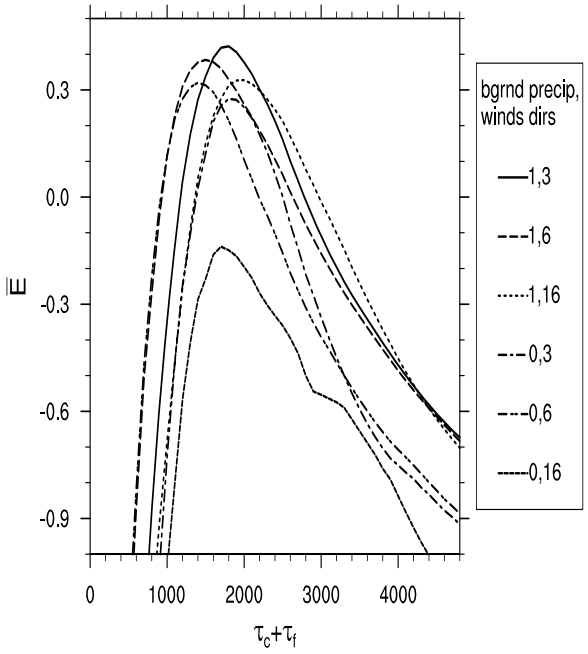

4. Combined Efficiency plotted against the total cloud delay time. In this plot, only the highest fractionation factors, background precipitation values of 0 and 1mm/day and wind statistics using 3, 6 and 16 directions are used. Note that the best results require a total cloud delay of about 1700 seconds.